J. Fluid Mech. (1996), *vol.* 324, *pp.* 199–222

The motion of solid particles suspended in viscoelastic liquids under torsional shear

By J. FENG† AND D. D. JOSEPH

Department of Aerospace Engineering and Mechanics and the Minnesota Supercomputer Institute, University of Minnesota, Minneapolis, MN 55455, USA

(Received 31 August 1995 and in revised form 30 April 1996)

This paper presents an experimental study of the behaviour of single particles and suspensions in polymer solutions in a torsional flow. Four issues are investigated in detail: the radial migration of a spherical particle; the rotation and migration of a cylindrical particle; the particle–particle interaction and microstructures in a suspension of spheres; and the microstructures in a suspension of rods. Newtonian fluids are also tested under similar flow conditions for comparison. A spherical particle migrates outward at constant velocity unless the polymer solution is very dilute. A rod in a viscoelastic fluid has two modes of motion depending on its initial orientation, aspect ratio, the local shear rate and the magnitude of normal stresses in the fluid. In the first mode, the rod rotates along a Jeffery-like orbit around the local vorticity axis. It also migrates slowly inward. The second mode of motion has the rod aligned with the local stream at all times; the radial migration is outward. A hypothesis proposed by Highgate & Whorlow (1968) on the radial force on a particle in a cone-and-plate geometry is generalized to explain the variation of migration speed in torsional flows. Spheres form chains and aggregates when the suspension is sheared. The chains are along the flow direction and may connect to form circular rings; these rings migrate outward at a velocity much higher than that of a single sphere. Rods interact with one another and aggregate in much the same way, but to a lesser extent than spheres. It is argued that the particle interaction and aggregation are not direct results of the shear flow field. Two fundamental mechanisms discovered in sedimentation are applied to explain the formation of chains and aggregates. Finally, the competition between inertia and elasticity is discussed. A change of type is not observed in steady shear, but may happen in small-amplitude oscillatory shear.

1. Introduction

Solid spheres and fibres are added to polymer melts to lower cost or to achieve desirable properties. In processing such composite materials, it has been observed that the solids tend to migrate across streamlines and form aggregates, and fibres exhibit complex orientation depending on the flow field. Thus, inhomogeneity and anisotropy occur in the finished product. For instance, solid concentration gradients develop in injection moulding of plastics filled with glass beads and short fibres (Kubat & Szalanczi 1974; Schmidt 1977; Hegler & Mennig 1985). This has been attributed to a host of causes including inertia, viscoelastic normal stresses and special velocity profiles near the gate or stagnation points. Bright, Crowson & Folkes (1978) and Toll & Andersson (1993) described complicated patterns of fibre orientation in various parts

† Present address: Department of Chemical Engineering, University of California, Santa Barbara, CA 93106, USA.

of the moulded article. In extrusion of fibre-filled melts, Wu (1979) observed distinctive regimes at different flow rates. The surface of the extrudate becomes roughened with protruding fibres as the flow rate increases, and the fibre distribution in the extrudate and the shape of the cross-section vary accordingly. More recently, Becraft & Metzner (1992) observed similar regimes and examined many factors as possible mechanisms responsible for the transition between regimes. All the above results are qualitative in nature and the explanations are usually speculative. The main reason is that those studies strive to approximate the geometry and flow fields in polymer processing. The experimental conditions are often not well controlled and characterized and the results not quantitatively comparable. Besides, direct tracking of individual particles under these experimental conditions is impossible, thus rendering arguments on particle behaviour tentative.

Modelling of the flow of solid-filled polymers has attracted many ingenious researchers from the fields of polymer rheology and processing and fluid dynamics. Unfortunately, all models up to now fall far short of accounting for the solid behaviour mentioned above. Solid fibres are assumed to follow the Jeffery orbit (Jeffery 1922), which applies rigorously only to creeping flows of Newtonian fluids. Fibre–fibre interaction is modelled as a Brownian-like diffusion (Advani & Tucker 1987). Ait-Kadi & Grmela (1994) is the only work that allows for viscoelastic media: the extra stress of the fluid is given by a FENE-P model and the solid contribution to the stress is given by the Dinh–Armstrong equation (Dinh & Armstrong 1984) modified to include non-Newtonian effects on the drag. This is the most sophisticated model that we have seen. Yet by no means can fibre aggregation and migration be simulated because the nonlinear mechanisms for these scenarios are not understood.

Therefore, a wide gap exists between the complexity of flows under realistic processing conditions and the capability of continuum modelling. This points to the need for studying the mechanisms of particle migration and interaction by well-designed experiments. This task was first undertaken some 40 years ago by Mason and co-workers (Trevelyan & Mason 1951). In simple shear flows in a Couette device and Poiseuille flows in capillary tubes, the migration and rotation of single solid spheres, rods and liquid drops have been carefully studied. Viscoelastic normal stresses and inertia are identified as the nonlinear mechanisms for the intriguing behaviour of particles. For example, in a Poiseuille flow of a Newtonian fluid, a neutrally buoyant solid sphere migrates to a radial position roughly halfway between the centre and the wall (Segré-Silberberg effect). If the fluid is viscoelastic, however, the sphere will migrate to the centre of the tube (Karnis & Mason 1966; Gauthier, Goldsmith & Mason 1971*b*). A solid rod in a shear flow does not follow the Jeffery orbit indefinitely. Instead, the orbit evolves into one with maximum viscous dissipation in a Newtonian fluid and one with minimum viscous dissipation in a viscoelastic fluid (Karnis, Goldsmith & Mason 1966; Gauthier, Goldsmith & Mason 1971*a*, *b*). If the fluid has strong normal stresses and the shear rate is sufficiently high, the rod may align itself with the streamline (Bartram, Goldsmith & Mason 1975). Leal (1979, 1980) and Brunn (1980) have independently developed perturbation methods for weakly nonlinear flows. Their theories have successfully demonstrated that the leading-order effects of the slightest amount of inertia or normal stress indeed give rise to the respective behaviour observed.

More recently, Prieve and co-workers have carried out a series of experiments in a torsional flow between two parallel plates. A solid sphere migrates inward in a 1% polyisobutylene in polybuten solution; the radial velocity agrees with the perturbation theories (Karis, Prieve & Rosen 1984*a*). Later experiments using more dilute solutions

discovered a peculiar phenomenon (Karis, Prieve & Rosen 1984*b*; Prieve, Jhon & Koenig 1985; Choi, Prieve & Jhon 1987). The sphere may migrate in either direction depending on its initial position. A critical streamline is determined: spheres initially released inside the critical streamline migrate inward while spheres initially released outside migrate outward. More curiously, the velocity of radial migration does not vanish as the initial position of a sphere approaches the critical streamline. Instead, there is an apparent discontinuity in the radial velocity as the particle's initial position crosses the critical streamline. The anomalous motion of the sphere is believed to be caused by viscoelasticity. Obviously, the perturbation theories fail in this situation, so it is hard to understand how they have worked for the more concentrated solution used in the first paper (Karis *et al.* 1984*a*).

Interaction among spheres in sheared suspensions in viscoelastic liquids has been studied by a few authors. Highgate & Whorlow (1968) used a cone-and-plate rheometer to shear suspensions of spheres in polyisobutylene solutions. The spheres form rings of local high solid concentration and these rings migrate outward, leading to complete clearance of solid particles from the flow field. Michele, Patzold & Donis (1977) made suspensions of tiny glass beads in polyisobutylene and polyacrylamide solutions. A drop of the suspension was placed between two glass plates. The two plates were pressed together and one glass moved back and forth above the other. Such oscillatory shear causes the glass beads to form chains that are aligned in the flow direction. Giesekus (1981) further noticed in a bimodal suspension that these chains are selective in terms of particle size: the two species of spheres each form chains of their own. More recently, Petit & Noetinger (1988) observed similar structure in a suspension undergoing oscillatory shear driven by loudspeakers. We have found no experimental results on fibre–fibre interaction and aggregation in viscoelastic fluids.

The experiments to be reported here are inspired by the work of Prieve *et al.* (1985). We generate a torsional flow by rotating one circular disc above another that is stationary. Polymer solutions and Newtonian fluids are used as suspending media. Four topics are studied:

(*a*) The migration of a single sphere in the torsional flow. Because the intriguing results of Prieve *et al.* (1985) cannot be explained by any theory, confirmation using different fluids and parameters is warranted. Our results turn out to be somewhat different from theirs. In particular, the critical streamline is not found. This may well be due to limitations in our device and test materials.

(*b*) The migration and rotation of a single solid rod. As mentioned before, the rotation and orbit evolution of rods in Couette and Poiseuille flows have been studied. We have found that the orbit evolution in a torsional flow is essentially the same as in a simple shear flow. The rod, however, migrates inward or outward depending on its mode of motion.

(*c*) Sphere–sphere interaction and aggregation. Though Giesekus (1981) mentioned studies done at Dortmund using torsional flows, we have not seen such results in the literature. Our work appears to be the first well-controlled experiment using continuous shear. We note that even the simplest scenario of particle–particle interaction cannot be explained in the framework of perturbation theory (Brunn 1980). Thus, the experiments will provide us with new insights into the fully nonlinear nature of the interactions.

(*d*) Interaction and aggregation of rod-like particles. We have found that rods aggregate under shear in a similar way, but to a much lesser extent than spheres.

Admittedly, the results reported may not apply directly to explain phenomena encountered in polymer processing. We will try, however, to extract the basic fluid

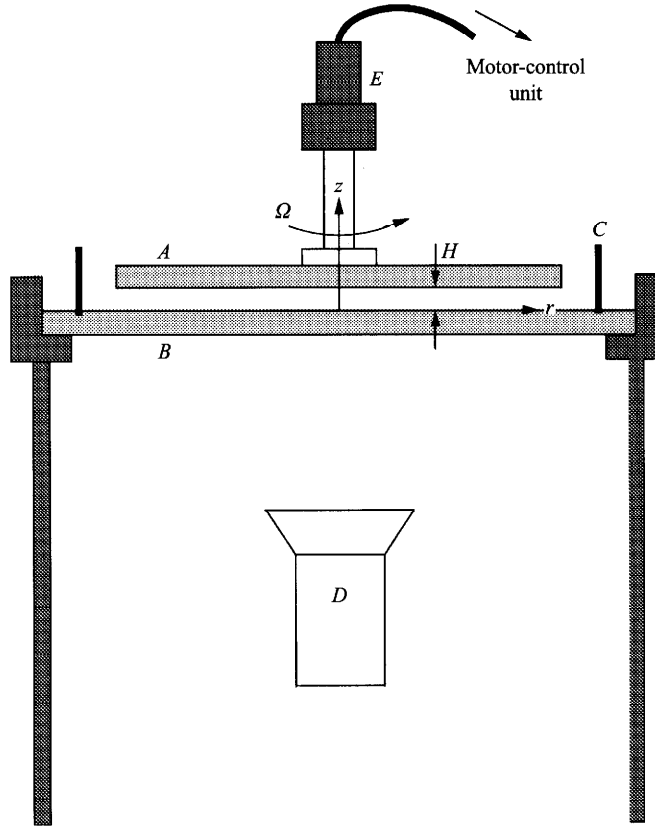

FIGURE 1. A sketch of the experimental setup.

dynamics governing particle motion and interaction in viscoelastic fluids. A better understanding of these mechanisms will undoubtedly benefit the effort to model the flow and processing of such materials, and eventually help to improve industrial processes.

An outline of the paper is as follows. Section 2 describes the equipment and procedure used in the experiments. Experimental results are presented in §3. In §4 we explore the mechanisms underlying the observed behaviour. A summary of results is given in §5.

2. Apparatus and procedure

Figure 1 is a sketch of the experimental setup. A is a glass disk of diameter 22 cm and thickness 0.5 cm. It is glued to an aluminium shaft that is clamped onto a drill press; thus A can be moved up and down by a control handle. The rotation of A is driven by a step motor E mounted on top of the modified drill press and the speed of rotation Ω can be changed easily using a motor-control unit. B is another glass disk of the same thickness but a larger diameter. Concentric circles are printed on a transparency sheet and glued on the bottom of B. A short aluminium cylinder C is glued onto B; the gap between the edge of A and the inner surface of C is 0.5 cm. D is a video or photo camera. The gap H between A and B can be measured with an accuracy of 0.01 mm.

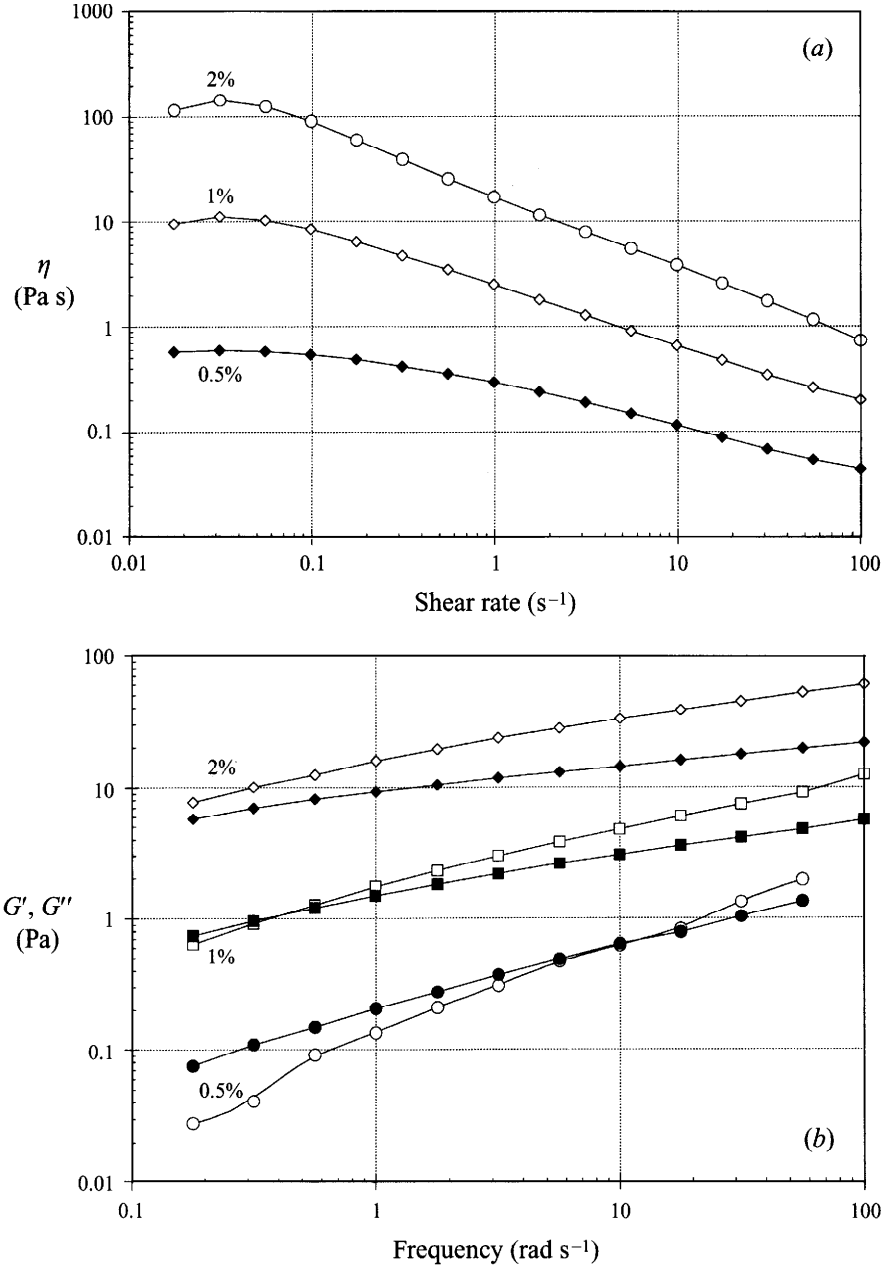

FIGURE 2. The rheological properties of polyox solutions. (*a*) Shear viscosity and (*b*) dynamic moduli. Open symbols represent G' and filled ones G''.

Before each experiment, the bottom plate B is levelled to within 0.07 mm at the rim, and A is aligned with B to within 0.07 mm at the rim. Then A is raised and the sample fluid is loaded onto B. A is then lowered to the desired gap size. Air bubbles trapped in the liquid are sucked out using a syringe needle through a re-sealable hole on the shroud C. Single spheres and rods are injected through the same hole to a specific radial and vertical position. After the shear is started, trajectories of single particles are recorded onto video tapes and later read by use of a VIA100 reticle unit. The maximum

error in the radial position of the particle is 0.2 mm. The parallax error is estimated to be negligible. When suspensions of many particles are sheared, we use a photographic camera coupled with close-up lenses to capture the details of the particle interactions.

The viscoelastic liquids used are aqueous solutions of poly(ethylene oxide) (Polyox WSR301 from Union Carbide) of different concentrations. These solutions exhibit large normal stress differences and have a strong storage modulus (Joseph *et al.* 1994). Figure 2 shows the rheological behaviour of 2%, 1% and 0.5% solutions. We have used glycerin and Newtonian silicone fluids (Dow 200 fluids) in certain tests as a comparison with the polymer solutions. Polystyrene spheres with diameters ranging from 250 to 850 μm are used. The density of the material is 1.05 g cm^{-3}. Rod-like particles are cut from two kinds of plastic threads with density 1 and 1.26 g cm^{-3}, respectively. The first density roughly matches that of polyox solutions and silicone oils while the second matches that of glycerin. The diameter of the rods ranges from 120 to 330 μm and the length from 0.5 to 4 mm.

3. Experimental results

All experiments are done in a temperature-controlled room, and no further remedies are taken to counter viscous heating. We repeatedly measured the temperature of the liquid before and after one hour of shearing at a typical shear rate. The temperature rise is never over 1 °C. Mechanical degradation is minor in our tests because the shear rate is low ($\sim 20\ s^{-1}$) and the sample is used no longer than a week.

3.1. *Secondary flow*

It is well known that secondary recirculations occur in the parallel-plate type of apparatus (Savins & Metzner 1970; McCoy & Denn 1971), and that inertia and viscoelastic normal stresses cause opposite vortical flows (Hill 1972). In our apparatus, the intensity of secondary flow is expected to depend on the gap size H and the angular velocity of the upper plate Ω. In a preliminary test we inject a polystyrene sphere of diameter $d = 610$ μm and a glass sphere with $d = 850$ μm at different radial and vertical positions. The fluid is 2% polyox solution, and the plates are separated by $H = 4$ mm. Then the upper plate starts to rotate at $\Omega = 6.8$ r.p.m. If we assume that the particle follows the local fluid, the angular velocity ω with which the particle revolves indicates its elevation z. The polystyrene sphere is almost neutrally buoyant and it moves away from each plate toward the midplane $z = H/2$, while at the same time migrating outward. The glass sphere is considerably heavier than the fluid and it adopts a vertical position close to the bottom plate. Interestingly, it migrates inward. This points to a secondary flow that goes inward near the stationary plate, which is apparently caused by inertia.

This secondary flow can be suppressed by reducing H or Ω. So we repeated the above procedure using $H = 2$ mm and $\Omega = 3.8$ r.p.m. Both glass and polystyrene spheres rapidly approach the midplane, and their radial migrations are both outward. Since the narrow gap does not permit the glass sphere to stay low, this cannot prove the absence of secondary flow. For this purpose, a small blob of blue ink is injected at $r = 6$ cm near the upper plate while a blob of red ink is injected at $r = 8$ cm near the lower plate. Then the fluid is sheared at $\Omega = 4$ r.p.m. for one hour. Though two colour bands emerge as a result of diffusion, no radial displacement is discernible for either band. Thus, we are quite confident that secondary flow is not a factor in tests using the 2% solution with $H \approx 2$ mm and $\Omega \leqslant 4$ r.p.m.

To estimate the magnitude of secondary flows, Karis *et al.* (1984*a*) used an

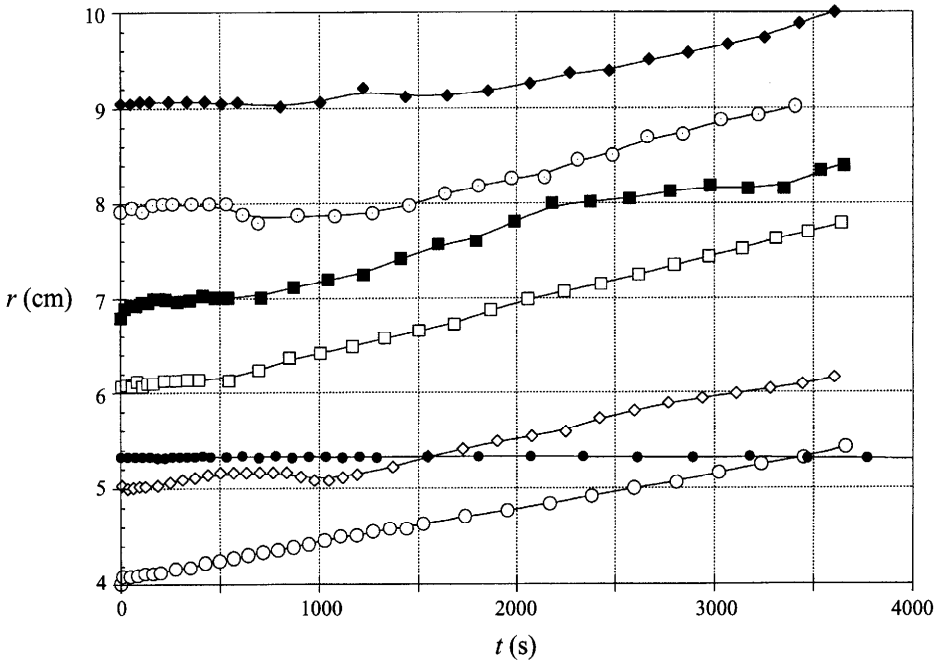

FIGURE 3. Radial migration of spheres in 2% polyox solution. The diameter of the sphere $d = 580$ μm. $H = 2$ mm, $\Omega = 2.55$ r.p.m. Also shown is the radial motion of the same sphere in a silicone oil (filled circles).

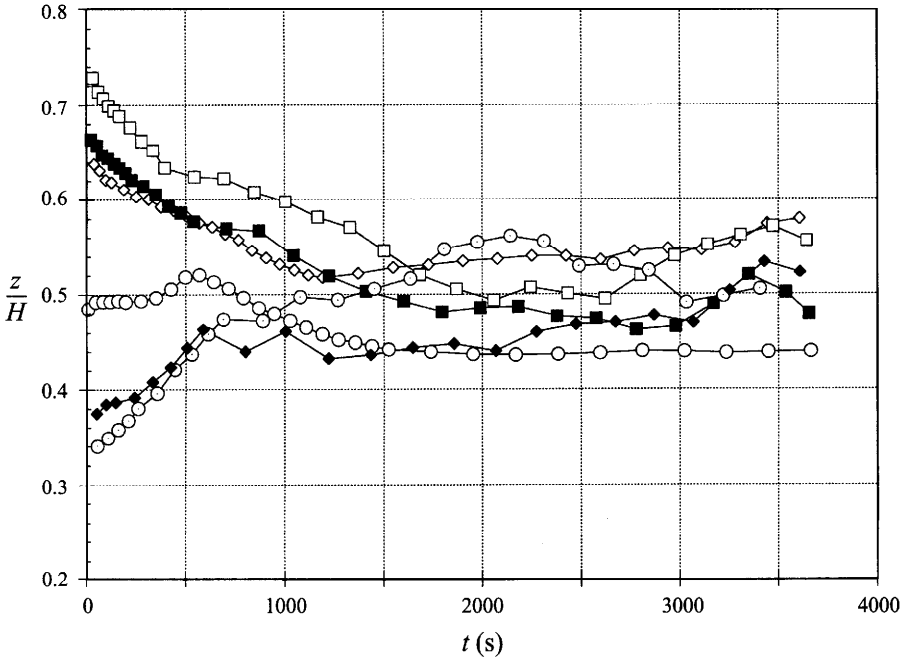

FIGURE 4. The vertical position of spheres in 2% aqueous polyox as inferred from their speed of revolution. Symbols correspond to those in figure 3.

asymptotic formula derived for low-Reynolds-number flows of Newtonian fluids. The radial velocity thus calculated was claimed to be much smaller than the observed migration speed in the viscoelastic solution. We double-checked this by putting their experimental parameters into the formula, and we obtained a radial velocity that is of the same order of magnitude as the migration velocity that they measured. Our speculation is that the inertia-induced recirculation was cancelled by that due to normal stress. This results in a negligible secondary flow, consistent with the observation that the radial migration does not depend on the elevation z of the particle.

3.2. *Radial migration of a sphere*

A sphere released in a 2% polyox solution migrates outward, and the radial velocity does not vary significantly with the radial position. Figure 3 shows a group of trajectories. Most of each trajectory falls on a straight line, and its slope does not depend on r in a systematic way. The initial portion of most trajectories, however, does not fall on the same straight line. By studying the vertical elevation of the particle we realized that this is caused by the proximity of the plates. If the particle is initially released close to one of the plates, it goes toward the midplane (figure 4). At the same time, its radial motion takes the form of outward migration followed by a plateau or even a slight inward migration. By then the particle is near the midplane and will migrate outward at a constant speed. The exact mechanism for this initial episode is not clear. It is not related to any secondary motion because the pattern is the same for particles released near the upper or lower plate. for particles released near the midplane, this does not happen; the particle starts to migrate outward at a constant velocity as soon as it is released.

Also shown in figure 3 is a trajectory of the same sphere in a 4000 CSt silicone oil. The viscosity of the oil matches that of the 2% polyox solution at the shear rate that occurs near $r = 5$ cm for the H and Ω values used. No radial migration is detected in two hours of shearing. This proves that the radial migration in the polyox solution is an effect of viscoelasticity.

The effect of the sphere's size on its migration velocity is illustrated in figure 5. For $d < 630$ μm, larger spheres migrate faster as expected. The trend is reversed for $d > 630$ μm. This is believed to be an effect of the hindrance of the plates when d/H becomes sufficiently large.

The results shown in figure 3 are quite different from the observations of Karis *et al.* (1984*b*) and Prieve *et al.* (1985). We obtained only outward migrations, and the radial velocity does not depend on the radial position r. Prieve *et al.* (1985) observed inward and outward migrations separated by a critical streamline, and the absolute value of the radial velocity increased linearly with r inside and outside the critical radius. The liquid used here is shear-thinning and that used by Prieve *et al.* has a nearly constant viscosity in the range of shear rate covered. The role of shear-thinning in the dependence of v_r on r will be further discussed in §4. Choi *et al.* (1987) suggested that the critical shear rate is related to the relaxation time of the fluid such that the critical radius would be larger for more dilute solutions. In our device the smallest radius observable on the plate is $r = 3$ cm, inside which the shaft prevents visual observation. It is possible that our 2% is too concentrated for the inward migration to be recorded, and so we repeated the tests in figure 3 with 1% polyox solution.

Because of the reduced viscosity of the 1% solution, lower angular velocity Ω has to be used lest secondary recirculation develops between the plates. On the other hand, if Ω is too small, the radial migration becomes very weak and hard to measure. Figure 6 shows some typical trajectories in 1% polyox solution. Still no inward migration is

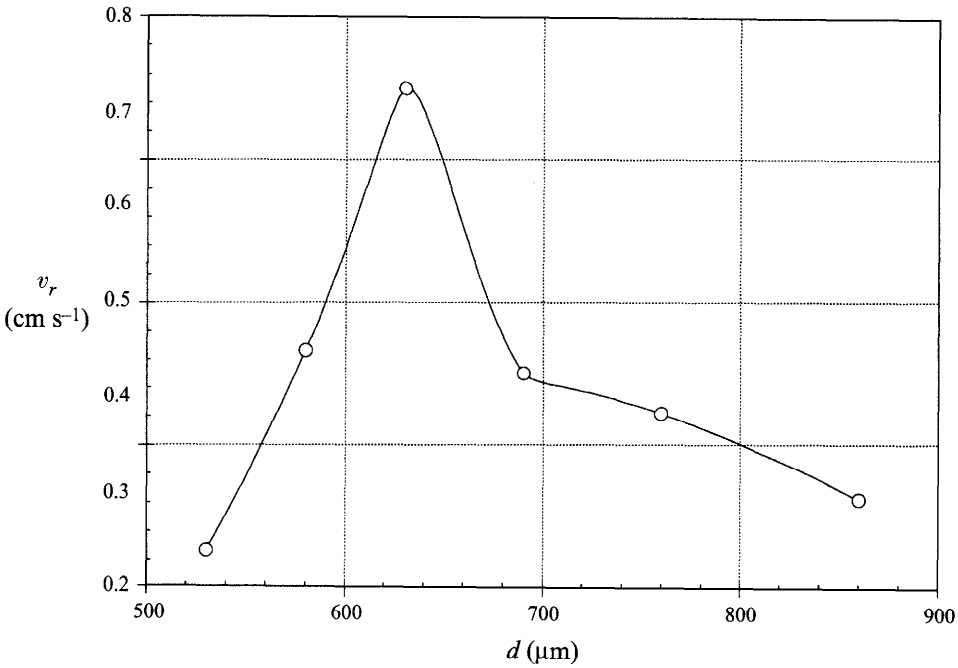

FIGURE 5. The radial velocity of a sphere in 2% polyox solution as a function of its diameter. $H = 2$ mm, $\Omega = 3.5$ r.p.m.

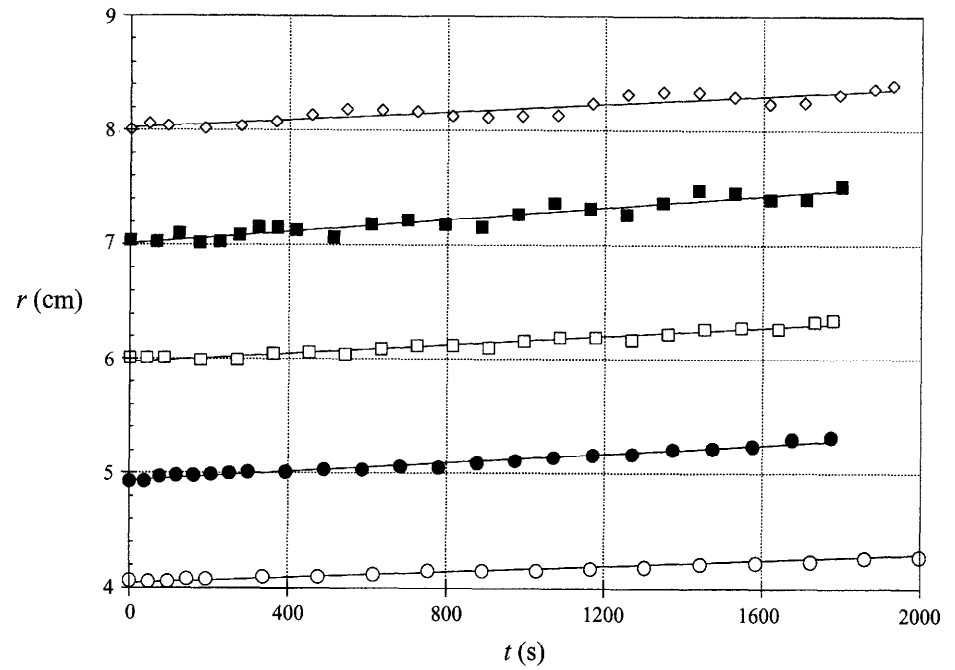

FIGURE 6. Radial migration of spheres in 1% polyox solution. The diameter of the sphere $d = 630$ μm. $H = 2$ mm, $\Omega = 2.8$ r.p.m.

observed. The velocity of migration, if scaled by ΩR (R is the radius of the upper disk), is about one half of that in the 2% solution for a sphere of the same size.

Testing using even more dilute solutions becomes very difficult because even smaller Ω has to be used. Also, because the particle is slightly heavier than the fluid, it settles to a position close to the bottom, where inertia-induced recirculation could also produce inward migration. To avoid this ambiguity, we added glycerin to the 0.5% solution to make it slightly heavier than the sphere. This way, the particle floats toward the upper plate and any inward migration can be attributed to viscoelastic effects. Results obtained in this fluid are less repeatable than in the other two solutions. Qualitatively speaking, slow inward migration occurs at all radial positions with a radial velocity on the order of 5×10^{-5} cm s^{-1}. This seems to agree with the arguments of Choi *et al.* (1987). We cannot confirm the existence of critical streamlines and the discontinuous migration velocity reported by Karis *et al.* (1984*b*).

3.3. *Rotation and migration of rod-like particles*

First we use glycerin to study the behaviour of a rod in a Newtonian fluid. Plastic rods of diameter $d = 170$ μm are cut into arbitrary length from a filament. The density of the rods matches that of glycerin closely.

Unless the rod is initially placed very close to one of the plates, it rotates as if along a Jeffery orbit (Jeffery 1922). The rotation evolves into a preferred orbit with the rod tumbling in the vertical plane, which corresponds to an orbit constant $C = \infty$ (Karnis *et al.* 1966). The rod spends most of the period aligned with the local streamlines and then flips every half period. No radial migration is observed. The evolution of the orbit is evidently a result of inertia and has been extensively studied for linear and quadratic shear flows (Karnis *et al.* 1966).

It is interesting to compare the measured period of rotation with the theoretical result of Jeffery. To do this, we use the empirical correlation of Anczurowski & Mason (1968) to convert the aspect ratio of a cylindrical rod r_p into that of an effective spheroid r_e:

$$r_e = 1.125 r_p^{0.78}.$$

For a rod of length $L = 1.2$ mm, the aspect ratio is $r_p = 7.06$. This gives $r_e = 5.16$. Given the radial position of the rod, the local shear rate $\dot{\gamma}$ can be calculated. Then the Jeffery period calculated from

$$T_j = \frac{2\pi}{\dot{\gamma}}(r_e + r_e^{-1}) \tag{1}$$

is 1.51 s. The measured period is $T = 2.37$ s, about 57% larger than the Jeffery period. For a longer rod ($L = 4$ mm, $r_p = 23.5$), the actual period is 84% larger than the Jeffery period. This discrepancy is readily explained by the wall effect. Ivanov, van der Ven & Mason (1982) noticed in Couette flows that small gap sizes causes slower rotation and prolonged period for long particles. This effect is particularly strong if the ends of the particle are not smooth, as is the case for our cylindrical rods. In addition, if the length of the particle exceeds the gap size, the particle is forced away from its preferred orbit and has to rotate while slanted. This is what we observed with the longer rod in our experiment. The prominent wall effects in Ivanov *et al.* (1982) and our experiment seem to contradict the numerical results of Ingber & Mondy (1994), which showed little increase in the period of a spheroid or a rod when the length of the particle exceeds half of the channel width.

If the neutrally buoyant rod is initially placed adjacent and more or less parallel to

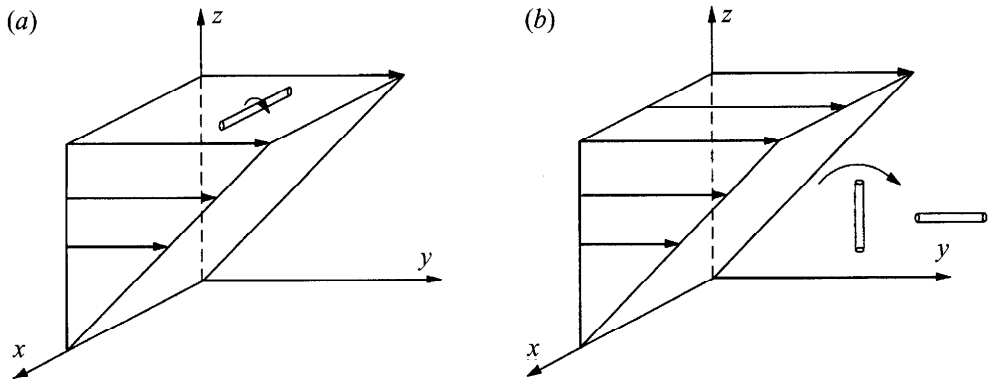

FIGURE 7. Preferred modes of motion of a rod in a simple shear flow. (*a*) Steady rolling in a plane of uniform flow is unstable in a Newtonian fluid unless kept in the plane by external force; (*b*) a rod tumbling in the vertical plane is the preferred orbit in a Newtonian fluid.

either plate, a completely different behaviour obtains. The rod stays in the horizontal plane and turns to a radial orientation, with its length perpendicular to the local streamlines. Then it rolls steadily. This happens to rods of all aspect ratios we tested. If a non-neutrally buoyant rod is introduced into the torsional flow at any point, it drifts toward one of the plates and then also adopts the 'cross-the-stream' orientation and rolls steadily.

This behaviour offers insight into the role of inertia in selecting the stable mode of motion in viscous fluids. In sedimentation and fluidization, it is well known that a long particle puts its long side perpendicular to the flow (Huang, Feng & Joseph 1994). Yet in shear flows, the preferred orbit affords maximum alignment with the streamlines. The key lies in that a rod of finite thickness lying in the (x, y)-plane is an unstable configuration (figure 7*a*). Given any three-dimensional disturbance, the rod will assume a Jeffery orbit, rotating on a cone surface. Inertia makes the cone fatter and eventually the rod tumbles in the (y, z)-plane (figure 7*b*). If the rod is forced, however, to stay in a horizontal plane by external agents, such as a solid wall in our case, the Jeffery rotation cannot prevail. Since the rod rolls with an angular velocity that equals about half of the shear rate (Feng, Hu & Joseph 1994), there will be a relative velocity locally between the fluid and the surface of the rod. Then the inertial effect is manifested by the familiar stagnation pressure that turns the rod perpendicular to the flow (figure 7*a*). For a neutrally buoyant rod, this configuration is perhaps only temporary: inertia gives rise to a repulsion force between the rod and the nearby wall (Feng *et al.* 1994). Thus, the rod will eventually shift away from the plate and again fall victim to three-dimensional disturbances. This will not happen, of course, to non-neutrally buoyant particles which will be kept close to one of the plates all the time.

In 2% polyox solution, we have found two modes of motion for a rod, depending on the local shear rate, the initial configuration and the rod's aspect ratio. The first mode occurs only if the shear rate is low and the rod is initially oriented close to the radial direction. Then the rod executes an oscillating motion along a Jeffery orbit around the local vorticity vector. Previous experiments in Couette flows (Gauthier *et al.* 1971*a*) suggested that viscoelasticity would drive the rod into a preferred Jeffery orbit with its axis completely aligned with the vorticity vector (orbit constant $C = 0$). In our experiment, the rod is initially assigned an orbit close to the preferred one. In the time of observation (typically 10 min), the rod seems to maintain the same orbit and no evolution is detected. Perhaps, inertia has prevented complete evolution and

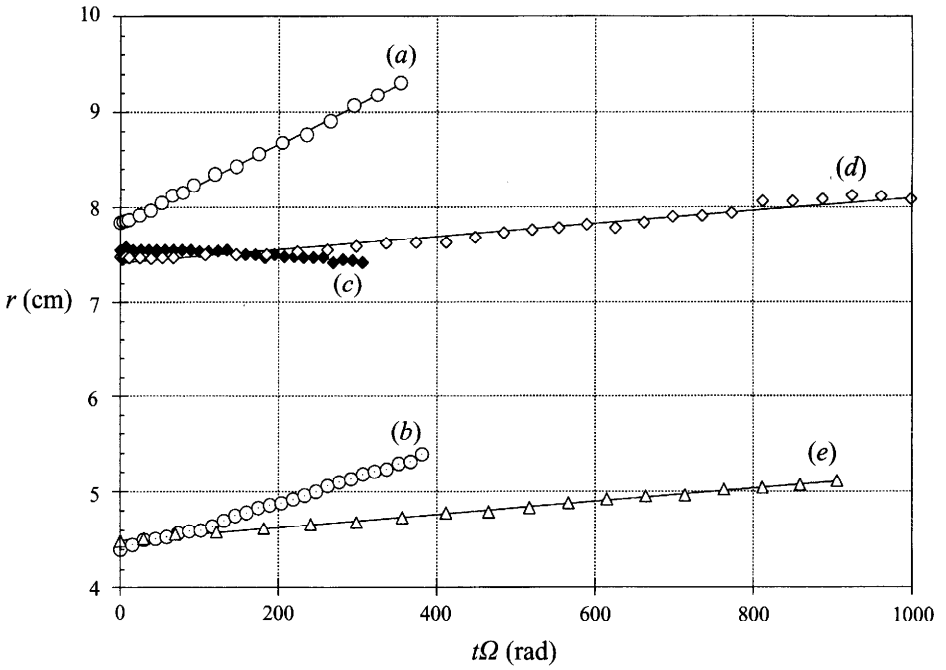

FIGURE 8. Radial migration of neutrally buoyant rods in polyox solutions. $H = 2$ mm. (*a*) The length and diameter of the rod are $L = 1$ mm and $d = 330$ μm. $\Omega = 3.9$ r.p.m. Aligned motion in 2% solution with radial velocity $v_r = 1.67 \times 10^{-3}$ cm s^{-1}. (*b*) Same as (*a*) except for a different initial position; $v_r = 1.03 \times 10^{-3}$ cm s^{-1}. (*c*) Same as (*a*) except that the rod is in oscillating motion. $\Omega = 1.6$ r.p.m., $v_r = -7.71 \times 10^{-5}$ cm s^{-1}, $C \approx 0.1$. (*d*) Same as (*a*) but the rod is longer $L = 1.8$ mm; $v_r = 2.81 \times 10^{-4}$ cm s^{-1}. (*e*) Same as (*b*) but in 1% polyox solution; $v_r = 2.82 \times 10^{-4}$ cm s^{-1}.

forced an equilibrium orbit close to $C = 0$. For a rod of aspect ratio $r_p = 5.45$, the period of the rotation is 4–8 times as large as the theoretical value of the Jeffery orbit. The discrepancy seems to be larger at higher shear rates, and is much larger than in glycerin.

If the same rod is initially oriented such that it makes a relatively large angle with the local vorticity, or if the shear rate is high enough, the rod immediately aligns itself with the local streamline upon start of the flow. Then it will stay aligned and be carried along by the flow. This is the second mode of motion, or 'aligned motion'. Rods with larger aspect ratios align with the flow more easily. For instance, a thin rod with $L = 1.8$ mm and $r_p = 10.6$ aligns immediately with the flow at the smallest shear rate tested in our device (~ 1.8 s^{-1}), even if it is carefully oriented in the radial direction before the shear starts.

The same two modes of motion have been observed in 1% polyox solution; all qualitative features of the motion are the same. The oscillating motion, however, persists up to higher shear rates than in the 2% solution; the oscillation also achieves larger amplitude. In addition, the period of rotation is shorter and closer to the theoretical value (equation (1)). These differences are consistent with the fact that rheologically the 1% solution is between a Newtonian fluid and the 2% solution.

To summarize, the oscillating motion prevails only if the shear rate and initial orientation fall into a small window. This window is affected by the aspect ratio of the rod and the properties of the fluid. Larger aspect ratio and larger normal stresses tend to shrink the window, though it is not clear whether it can be completely eliminated.

The behaviour of a rod in a torsional flow appears to be qualitatively the same as in a Couette flow (Karnis & Mason 1966; Gauthier *et al.* 1971*a*). The perturbation analyses of Leal (1975) and Brunn (1980) showed that the second normal stress difference causes an orbit drift toward $C = 0$. When the shear rate is sufficiently large, a steady solution emerges with the rod aligned with the flow. The rod selects one of the two solutions based on its initial orientation. This picture is entirely consistent with our findings. On may also note the interesting contrasts between Newtonian and viscoelastic fluids. Inertia leads to either (*a*) a tumbling motion that is 'aligned' with the flow or (*b*) a steady rolling that is perpendicular to the flow. Normal stresses lead to either (*c*) an aligned motion or (*d*) an oscillating motion that is 'perpendicular' to the flow. (*a*) and (*d*) resemble the basic Jeffery motion and can be derived theoretically by perturbing the Jeffery orbit (Leal 1980). (*b*) and (*c*), on the other hand, are caused by another form of the nonlinear effects.

Radial migration is observed for rods in viscoelastic fluids, being inward if they are in the oscillating mode of motion and outward if the aligned mode prevails. In both cases, rods migrate at a constant radial velocity v_r (figure 8). For outward migration (curve *a*), the non-dimensional radial velocity $v_r/\Omega R$ is about 8 times larger than that for inward migration (curve *c*). The outward migration is slower for a longer rod (curve *d*). This is somewhat surprising since a rod seems to migrate much faster than a sphere of the same diameter (cf. figure 3 and curve *a* in figure 8). In 1% polyox solution, v_r is about 1/4 of that in the 2% solution, other conditions being the same (curve *e*). In both modes of motion, the angular velocity with which the rod revolves around the hub approaches $\Omega/2$, indicating that the rod drifts vertically to the midplane between the plates.

3.4. *Behaviour of a suspension of spheres*

Polystyrene spheres are added to 2%, 1% and 0.5% aqueous polyox to form suspensions. The diameter of the spheres ranges from 250 to 850 μm; we used the particles directly out of the bottle and the size distribution is unknown. The solid volume fractions used are 2%, 5% and 10%.

Once the flow starts, spheres interact with one another and microstructures form. The characteristics of this process are the same for suspensions of various solid fractions in different solutions. Figure 9 shows a sequence of snapshots of 2% spheres in 2% aqueous polyox. Black lines in the background are portions of concentric circles on the lower plate; the flow direction is from bottom to top in the photographs.

Shortly after the shear starts, spheres near the outer edge, where the shear is strongest, start to form short chains that are aligned to the flow. Such chains appear throughout the suspension after 2 min of shearing (figure 9*b*). In this picture, the chains are composed mostly of larger spheres. After 8 minutes of shearing (figure 9*c*), the chains have connected to form longer strings. Neighbouring chains apparently attract each other and they aggregate to make the string thicker. It may also be noticed that smaller spheres start to form their own chains. This size selection in particle–particle interaction agrees with previous observations of Giesekus (1981). In figure 9(*d*), the strings have further grown in length and thickness, and become complete circular rings. These rings continue to absorb short chains until only a few spheres are left in the clear liquid between adjacent rings (figure 9*e*). Figure 9(*f*) gives a view of the entire flow field after 20 min of shearing.

The rings migrate outward; the interior of the flow field will be depleted of all solids in a certain time. One might expect spheres of different size to migrate at different speed, therefore causing disintegration and regrouping of rings. This does not happen. Most rings survive the migration and reach the rim as a whole. Occasionally, a thin ring

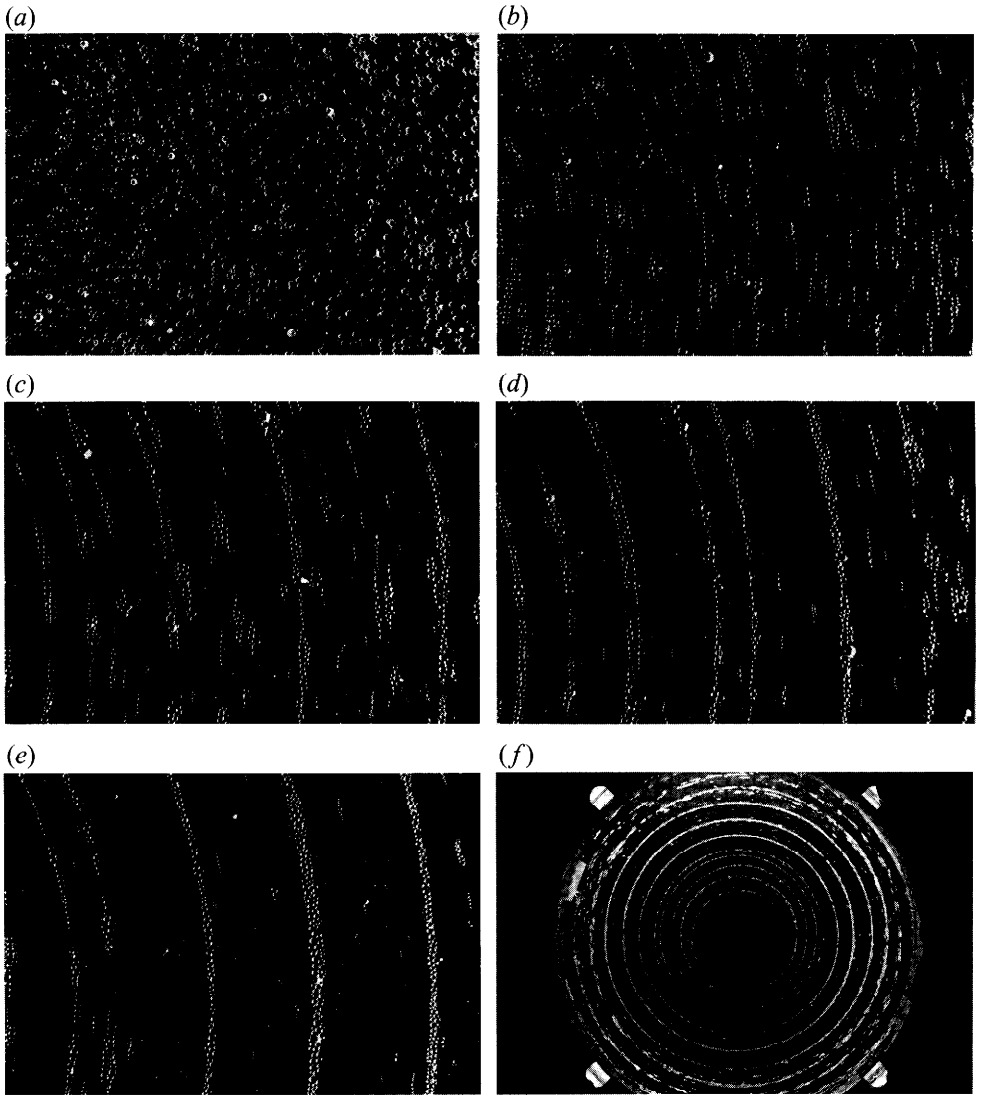

FIGURE 9. Formation of microstructures in 2% suspension of spheres in 2% aqueous polyox. $H = 2.1$ mm. (*a*) Initial state; (*b*) after 2 min of shearing at $\Omega = 3.5$ r.p.m.; (*c*) after 8 min; (*d*) after 12 min; (*e*) after 18 min; (*f*) an overview of the rings after 20 min of shearing.

breaks up as its diameter grows. Then all spheres will be absorbed by the next ring; no dispersion of spheres is observed. When rings first appear, they are more or less evenly spaced. After the first few rings on the outside have arrived at the rim, the ring spacing on the inside grows. After the solid concentration has dropped considerably near the hub, thinner rings emerge. They are also closer to one another (cf. figure 9*f*). The rings rotate at roughly half the speed of the upper plate, suggesting that they prefer a vertical position midway between the plates.

The radial migration of rings is measured in one case using 10% solids in 2% aqueous polyox. Figure 10 shows the migration of two rings: (*a*) is a thick ring that appears at an early stage and (*b*) is one of the thin rings that appear later. Ring (*a*) starts with a high speed and then settles at a lower speed $v_r = 8.68 \times 10^{-4}$ cm s^{-1}. The

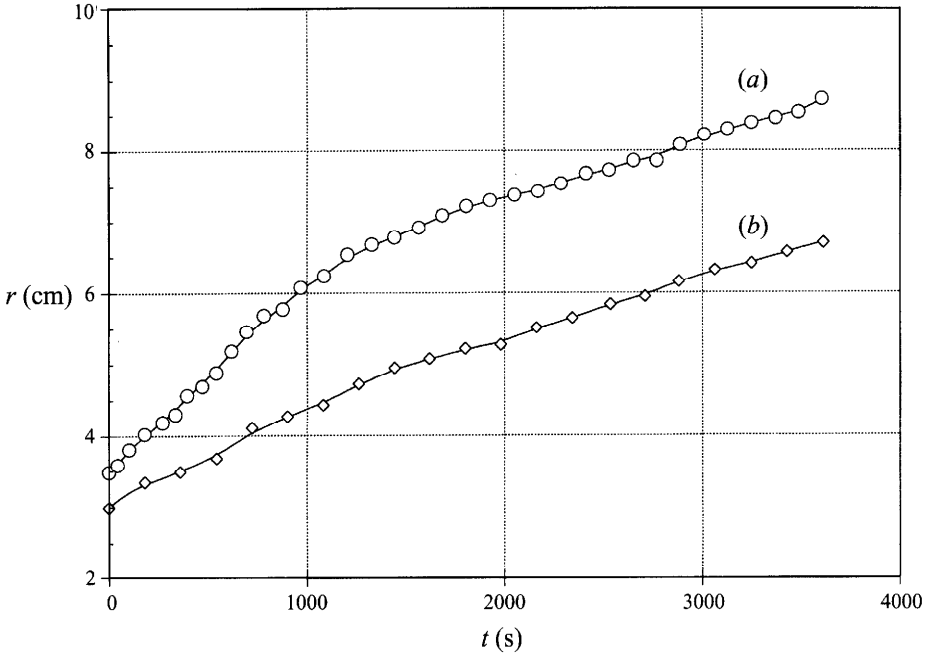

FIGURE 10. The outward migration of rings in 10% suspension of spheres in 2% aqueous polyox. $H = 2.1$ mm, $\Omega = 3.5$ r.p.m. Ring (*a*) is a thick ring that appears in an early stage and (*b*) is one of the thin rings that appear later; the time has been shifted for comparison.

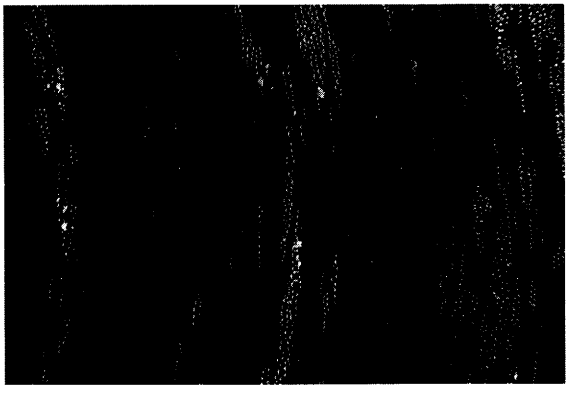

FIGURE 11. Rings give way to wider and shorter aggregates after 2 min of stronger shear at $\Omega = 15.7$ r.p.m.

entire trajectory can be seen as two segments of straight lines joined at $t \approx 1000$ s. The same pattern holds for ring (*b*). Though its initial migration is slower, ring (*b*) later attains essentially the same velocity as (*a*) ($v_r = 8.40 \times 10^{-4}$ cm s^{-1}). Another intriguing feature of the migration is that rings, composed of spheres of various sizes, migrate much faster than a single sphere under the same shear (see figure 5).

We notice in figure 9(*f*) that the rings tends to break up as it approaches the outer edge. Two possible explanations are (i) the ring is stretched too thinly, (ii) the higher shear rate breaks the ring up. The first scenario appears unlikely since most segments of the broken ring are still thick, with three or four chains attached abreast. This

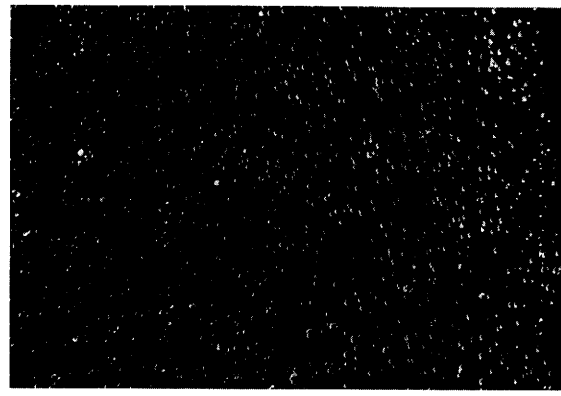

FIGURE 12. No microstructures appear in 2% suspension of spheres in a silicone oil. After 25 min of shearing at $\Omega = 3.5$ r.p.m., $H = 2.1$ mm.

prompted us to investigate the influence of shear rate on the ring structure. After 20 min of shearing at $\Omega = 3.5$ r.p.m., Ω is suddenly raised to 15.7 r.p.m. All rings are destroyed within a short time, and the segments join abreast to form aggregates that are relatively short and wide. Figure 11 shows a snapshot of these aggregates after 2 minutes of strong shear. After that, the aggregates undergo little morphological change.

Finally, to confirm that the microstructures are formed by viscoelastic stresses, we put suspensions of spheres in a silicone oil under the same shear. No signs of microstructure are found (figure 12).

3.5. *Behaviour of a suspension of rods*

Plastic rods of diameter $d = 170$–330 μm and length $L = 0.5$–4 mm are mixed with 1% polyox solutions. The mixture is stirred thoroughly and left still for a few hours to let the air bubbles out before being loaded on our parallel-plate device. Two suspensions of 2% and 5% solid volume fractions are studied and the behaviour is similar. Figure 13 shows a sequence of snapshots of the suspension.

After the flow starts, most rods align themselves with the flow direction in a few seconds. After 7 min of shearing at $\Omega = 5.75$ r.p.m. (figure 13*b*), some rods seem to have formed chains. But this is much less obvious than with the spheres (cf. figure 9*b*). Also unlike suspensions of spheres, the suspension of rods is still more or less homogeneous; no large aggregates of particles are found. Then the angular velocity of the upper plate is suddenly raised to $\Omega = 12.1$ r.p.m. At this high shear rate, rod chaining, aggregation and outward migration are all accelerated. After 9 min of shearing (figure 13*c*), more chains have formed and the suspension becomes non-homogeneous with aggregates of rods and areas of clear liquid. At this point, Ω is increased to 31.1 r.p.m. After 30 s of shearing (figure 13*d*), band-like structures can be discerned. Compared with the rings of figure 9(*e*), these structures of assembled rods are much less conspicuous; many thin chains and single rods fill the space between the aggregates.

We may conclude from figure 13 that rod-like particles align with the flow. They also associate with one another to form chains and aggregates. These interactions are much weaker than those among spherical particles.

For comparison, suspension of rods in a silicone oil has also been studied. Aside from frequent collision, each rod behaves much like the single rod studied in glycerin.

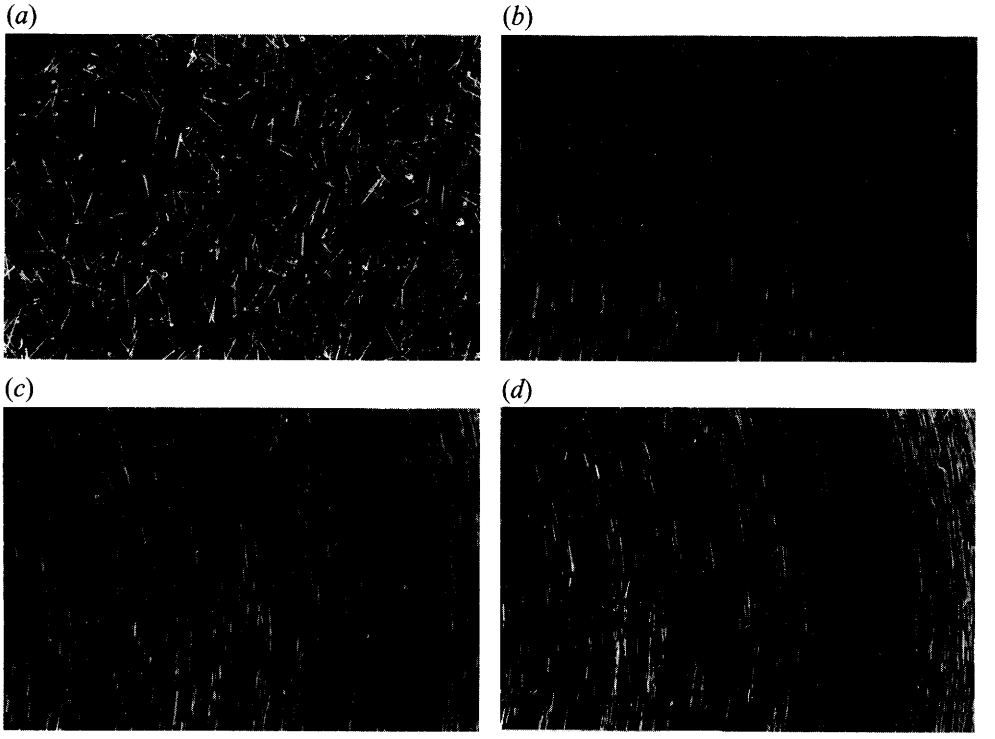

FIGURE 13. The formation of microstructures in 2% suspension of rods in 1% aqueous polyox. $H = 2.6$ mm. (*a*) Initial state; (*b*) after 7 min of shearing at $\Omega = 5.75$ r.p.m.; (*c*) after 9 min of shearing at $\Omega = 12.1$ r.p.m. following (*b*); (*d*) after 30 s of shearing of $\Omega = 31.1$ r.p.m. following (*c*).

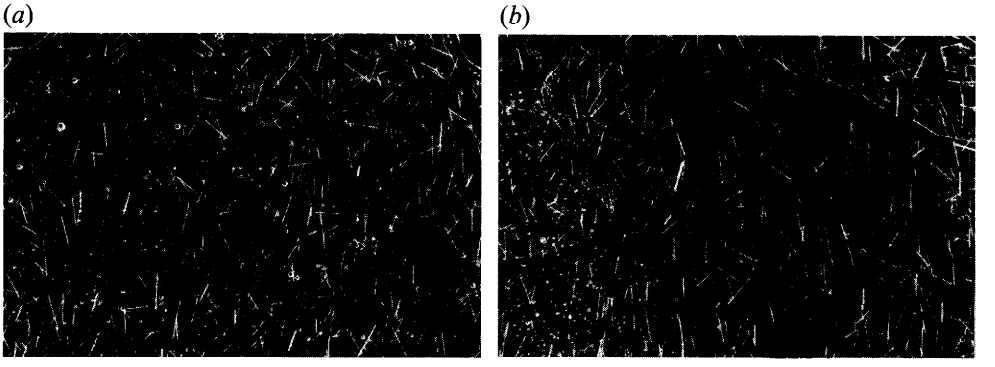

FIGURE 14. The behaviour of 2% rod suspension in a silicone oil. $H = 2.1$ mm. (*a*) Initial state; (*b*) after shearing at $\Omega = 6$ r.p.m. for 21 min.

They rotate as if along a Jeffery orbit, and the orbit slowly evolves into one in which the rod tumbles in the vertical plane. Some of the longer rods have to settle into lower orbits because of the restrictions of the solid walls. Because of this orbit evolution, a certain degree of alignment with the stream is achieved after long time of shearing (figure 14). The air bubbles migrate inward because of centripetal force.

4. Discussion

Two major results of this study are the migration of particles in a torsional flow and interaction and aggregation among particles. Obviously, complete interpretations of these phenomena are not yet available. In this section, we will try to piece together previous knowledge on these subjects and new insights gained in this work to form a better understanding of the mechanics.

Brunn (1976) and Chan & Leal (1977) have studied the motion of a sphere in a shear flow using perturbation methods. When applied to a torsional flow, the theory predicts an inward migration with radial velocity (Karis *et al.* 1984*a*)

$$v_r = -L\left(\frac{\Omega a}{H}\right)^2 r, \tag{2}$$

where

$$L = -\frac{5}{126}\frac{\alpha_{11}+11\alpha_2}{\eta}$$

is a positive material constant for a second-order fluid model:

$$T = \eta \boldsymbol{A}_1 + \alpha_2 \boldsymbol{A}_2 + \alpha_{11} \boldsymbol{A}_1 \cdot \boldsymbol{A}_1,$$

where $\boldsymbol{A}_1$ and $\boldsymbol{A}_2$ are the first- and second-order Rivlin–Ericksen tensor. Equation (2) has been verified by measurements of v_r in 1% w/w polyisobutylene in polybutene solution (Karis *et al.* 1981*a*). The perturbation theory apparently breaks down when Karis *et al.* (1984*b*) and Prieve *et al.* (1985) later used less-concentrated PIB (0.5% and 0.1% w/w) in a more viscous PB solvent. The shear rate is of the same order of magnitude in all three experiments. This appears anti-intuitive. The 2% polyox solutions used in this work have an elastic modulus that is more or less the same as that of the solution used in Karis *et al.* (1984*b*) (compare our figure 2 with their figure 4). Our results do not agree with equation (2).

Highgate & Whorlow (1968) proposed a simple hypothesis to explain the radial migration in a cone-and-plate device. If the flow is slow, fluid particles experience zero resultant force in the radial direction when orbiting along circular streamlines. The radial force due to normal stress differences is balanced by a pressure gradient. We remind the reader that, because of the curved streamlines, normal stresses do exert a radial force on a fluid particle even though the stresses are uniform in a cone-and-plate geometry. If a solid particle is introduced into the flow, the local disturbances will change both the normal stresses and the pressure. Thus the balance between the two is broken and a radial force arises. From intuition, Highgate & Whorlow assumed that this force is proportional to the pressure gradient in the undisturbed flow:

$$F_r \propto \frac{\mathrm{d}p}{\mathrm{d}r}. \tag{3}$$

It is easy to show that $\mathrm{d}p/\mathrm{d}r$ is proportional to r^{-1} in this flow field. If v_r is taken to be proportional to F_r, (3) leads to a radial velocity that is proportional to r^{-1}, which agrees approximately with their data. We will generalize this argument to show that the radial velocity measured in Karis *et al.* (1984*a*, *b*) and Prieve *et al.* (1985) and that measured here are also consistent with the hypothesis (3).

In a cone-and-plate device, the normal stress differences are uniform throughout the gap:

$$N_1 = \tau_{\phi\phi} - \tau_{\theta\theta} = \Psi_1 \dot{\gamma}^2,$$
$$N_2 = \tau_{\theta\theta} - \tau_{rr} = \Psi_2 \dot{\gamma}^2.$$

A radial force balance gives the pressure distribution (Bird, Armstrong & Hassager 1987, p. 522, note the different sign convention used therein):

$$p = -(\Psi_1 + 2\Psi_2)\dot{\gamma}^2 \ln\frac{r}{R} + p_a - \tau_{rr},$$

where p_a is the atmospheric pressure and τ_{rr} is an undetermined constant. The pressure gradient is therefore proportional to r^{-1}.

In a parallel-plate geometry, the shear rate is not uniform. This causes complications since little can be said of the normal stresses without invoking a constitutive model. By using the Criminale–Ericksen–Filbey equation, the pressure can be related to the normal stresses by (Bird *et al.* 1987, p. 526)

$$p(r) - p_a = \int_{\dot{\gamma}}^{\dot{\gamma}_R} (\Psi_1 + \Psi_2)\dot{\gamma}\,\mathrm{d}\dot{\gamma}, \tag{4}$$

where τ_{rr} has been put to zero. Ψ_1 and Ψ_2 are functions of the local shear rate defined by (see figure 1 for the geometry):

$$N_1 = \tau_{\theta\theta} - \tau_{zz} = \Psi_1(\dot{\gamma})\dot{\gamma}^2,$$
$$N_2 = \tau_{zz} - \tau_{rr} = \Psi_2(\dot{\gamma})\dot{\gamma}^2.$$

For many viscoelastic systems, the normal stress differences can be described by power laws in certain ranges of the shear rate (Bird *et al.* 1987). Now if we assume

$$\Psi_1 + \Psi_2 = K\dot{\gamma}^{-n},$$

it follows that

$$p(r) - p_a = \begin{cases} \dfrac{K\Omega^{2-n}}{(2-n)H^{2-n}}(R^{2-n} - r^{2-n}) & \text{if} \quad n \neq 2 \\ K\ln\dfrac{R}{r} & \text{if} \quad n = 2. \end{cases} \tag{5}$$

If the fluid behaves like a second-order fluid, Ψ_1 and Ψ_2 do not depend on $\dot{\gamma}$: $n = 0$. Then

$$\frac{\mathrm{d}p}{\mathrm{d}r} = -\frac{K\Omega^2}{H^2}r.$$

Applying the Highgate–Whorlow hypothesis (3) thus leads to

$$v_r \propto \frac{\Omega^2 r}{H^2}, \tag{6}$$

which agrees with equation (2) perfectly. We note that (6) also applies to later measurements of Karis *et al.* (1984*b*) and Prieve *et al.* (1985); the polymer solutions used do have a roughly constant Ψ_1 in $10 < \dot{\gamma} < 40\ \mathrm{s}^{-1}$.

If the fluid is shear-thinning such that $n = 1$, one gets

$$\frac{\mathrm{d}p}{\mathrm{d}r} = -\frac{K\Omega}{H},$$

which implies that the radial velocity v_r is independent of r. This is consistent with our measurements (cf. figure 3). Measurements of the first normal stress difference for 2% aqueous polyox shows a power-law region in $1 < \dot{\gamma} < 100\ \mathrm{s}^{-1}$ with $n = 0.98$. Bird *et al.* (1987) presented data for some other polymer solutions; both Ψ_1 and Ψ_2 seem to have

a power index $n \approx 1.4$ for intermediate ranges of $\dot{\gamma}$ of two to three decades. Incidentally, a sphere in a liquid with $n = 2$ in a parallel-plate geometry will migrate with $v_r \propto r^{-1}$ according to equation (5); this is similar to a sphere in a cone-and-plate device filled with any viscoelastic liquid. We emphasize that the above arguments do not indicate the direction of migration.

Choi *et al.* (1987) offered an interesting explanation for the critical streamline discovered by Karis *et al.* (1984*b*). The time scale t of the disturbance of the sphere is associated with the local shear rate. When the sphere is within the critical streamline, t is larger than the relaxation time of the polymer molecules, which thus behave as flexible molecules. On the other hand, rigid molecules are felt by a sphere that is outside the critical streamline; the sphere thus behaves differently. This argument seems to go along with the two-way migration of rods discovered in our experiment. A rod that is aligned with the flow perturbs the flow on a time scale $\dot{\gamma}^{-1}$, where $\dot{\gamma}$ is the local shear rate. A rod that is oscillating around the local vorticity axis perturbs the flow on a time scale of period T. Under our experimental conditions $T \gg \dot{\gamma}^{-1}$. This could explain why the aligned rod migrates outward whereas the oscillating one goes inward. We do not know of a continuum model that accommodates the transition in molecular reaction surmised by Choi *et al.* (1987). It appears similar to a change of type (Joseph 1990). A Deborah number and a Reynolds number may be defined by $De = \dot{\gamma}\lambda$ and $Re = \rho\dot{\gamma}d^2/\eta$, where λ and η are the relaxation time and viscosity of the fluid. Then a Mach number can be constructed:

$$M = (Re\,De)^{1/2} = \dot{\gamma}d\left(\frac{\rho\lambda}{\eta}\right)^{1/2} = \frac{\dot{\gamma}d}{c},$$

where c is the shear-wave speed. If a change of type occurs at the critical streamline ($M = 1$), the critical shear rate $\dot{\gamma}_c$ will satisfy

$$\dot{\gamma}_c\left(\frac{\lambda}{\eta}\right)^{1/2} = \text{const.}$$

In reality, Choi *et al.* (1987) discovered a different relationship: $\dot{\gamma}_c\lambda = \text{const}$. Hence, the proposed molecular transition does not fit into the framework of a change of type.

A robust feature of sheared suspensions in viscoelastic liquids is the chain structure aligned with the flow. Petit & Noetinger (1988) offered an explanation in terms of the secondary flow induced by the spheres' rotation. Since a rotating sphere in a viscoelastic fluid sucks in fluid around its equator and ejects fluid from its two poles, two spheres whose line of centres is parallel to the streamlines in a shear flow will attract each other. More spheres join in to form a chain. This theory is unlikely to be true for three reasons. First, it has been observed that once the spheres form a chain, they stop rotating (Michele *et al.* 1977). Hence rotation-induced suction cannot be the agent to hold the chain together. Secondly, the secondary flow implies repulsion between spheres rotating side by side. This cannot explain the rings made of several chains bundled together and the aggregates (figure 9). Finally, rod-like particles do not rotate but they do form chains and aggregates.

We believe that the mechanisms for particle–particle interaction and association are the same ones that operate in the sedimentation and fluidization of many particles in a viscoelastic liquid. Since all interactions happen on the plane of uniform velocity (cf. figure 7), the effect of shear is minimal. The two basic mechanisms found in sedimentation are: (i) attraction force between particles falling side by side (Joseph *et al.* 1994) or one on top of the other (Riddle, Narvaez & Bird 1977); (ii) preferred

orientation of a long particle in sedimentation with its long axis parallel to the direction of fall (Leal 1975; Liu & Joseph 1993).

Numerical simulations have revealed the anatomy of these mechanisms (Feng *et al.* 1995; Feng, Huang & Joseph 1996). Viscoelastic normal stresses cause a dramatic change in the pressure distribution near the particle. This new pressure field yields forces and torque that are opposite to those expected in a Newtonian fluid; the direct contribution of the normal stresses to the forces is relatively small. To be complete, we should mention that when the separation between two spheres falling one on top of the other exceeds a threshold value ($5d$–$10d$), a weak repulsion exists between them (Riddle *et al.* 1977; Feng *et al.* 1996). This should not affect the picture of particle aggregation in an important way.

Thus, if a suspension in viscoelastic liquids is sheared, particles attract each other in longitudinal and lateral directions. Primitive arrays made of spheres joined abreast will rotate until they too are aligned with the flow. Parallel chains attract each other and form thicker aggregates. Inhomogeneity develops just like in sedimentation (Joseph *et al.* 1994; Allen & Uhlherr 1989). Since thin rods aligned with the stream cause little disturbance to the ambient flow, the range of the lateral attraction force is much shorter for rods. Hence, fibre-like particles aggregate much more slowly (figure 13).

The above arguments address the effects of normal stresses alone. In reality, inertia will also be present and compete with normal stresses, in shear flow and sedimentation alike. Unlike normal stresses, inertia works differently in sedimentation and shear flows; this has been explained in §3.3. Thus, in a shear flow the competition may manifest itself as an orbit constant between 0 and ∞. This seems to be what we found in §3.3. Upon closer inspection, the data of Karnis & Mason (1966), Gauthier *et al.* (1971*a*, *b*) and Bartram *et al.* (1975) all show C decreasing for a rod in a viscoelastic fluid, but $C = 0$ is never observed. In sedimentation, the inertia–elasticity competition may assume a more dramatic form. The preferred orientation of a settling rod sees a rather abrupt change when its falling speed exceeds the shear wave speed in the liquid (Liu & Joseph 1993). The counterpart of this tilt transition in shear flows is a sudden change in the behaviour of a rod. It is aligned with the flow in the subcritical regime and will adopt a tumbling motion when a certain characteristic velocity exceeds the shear-wave speed. We tried to accentuate the inertial effects by increasing Ω (see §3.5). Rod aggregation and migration intensify, but no signs of a transition to tumbling motions were found (see figure 13). The shear-wave speed for 1% polyox solution is about 20 cm s^{-1}. The maximum velocity on the edge of the upper plate is 35 cm s^{-1}. The characteristic velocity for the flow around a particle, however, should be the slip velocity which tends to be very small. Then extremely large Ω is needed before a change of type happens. This was not further explored in our experiments.

A different situation arises when small-amplitude oscillatory shear is applied. Petit & Noetinger (1988) were able to generate chain structures of spheres that are perpendicular to the flow direction in a silicone oil. This resembles the stable across-the-stream arrays of larger spheres observed in water-fluidized beds (Fortes, Joseph & Lundgren 1987). A change of type may be achieved in a viscoelastic fluid using oscillatory shear. When the frequency f exceeds a certain value, the characteristic velocity, say fd, exceeds the shear wave speed of the fluid. Then chains of spheres aligned with the flow at lower frequency may break up and form chains that go across the streamlines. A similar transition can be expected for the orientation of rods.

5. Conclusions

The results reported in this paper may be summarized as follows:

(i) In a torsional flow of viscoelastic liquids, spherical and rod-like particles migrate radially under the action of normal stresses. The direction of migration depends on the properties of the fluid and the motion of the particle. The velocity of migration does not depend strongly on the radial position. These results, along with data in the literature, are consistent with a hypothesis proposed by Highgate & Whorlow (1968) on the driving force of the migration.

(ii) The rotation of a rod-like particle in a torsional flow is essentially the same as in a simple shear flow. This is true in both Newtonian and viscoelastic liquids.

(iii) Suspensions of spheres and rods in viscoelastic liquid exhibit microstructures under shear. Chains of particles align with the flow direction and aggregates of particles form at higher shear rate. Microstructures and inhomogeneity develop more readily for spheres than for rod-like particles.

(iv) The mechanisms for particle interaction and aggregation in shear flows are believed to be the same ones found in sedimentation: attraction forces among particles and preferred orientation of long particles.

(v) A change of type has not been observed in steady shear flow of viscoelastic liquids, perhaps because the rotation is too slow. A different kind of change of type may happen when small-amplitude oscillatory shear is applied.

This work was supported by the NSF, Fluid, Particulate and Hydraulic Systems, the US Army, Mathematics and AHPCRC, the DOE, Department of Basic Energy Sciences and the Schlumberger Foundation. J.F. acknowledges support from the Graduate School of the University of Minnesota through a Doctoral Dissertation Fellowship. We thank Dr R. Bai for his help with photography, Dr Y. J. Liu for assisting in rheological characterization of the samples, Dr A. Huang for reading the manuscript and offering criticisms and S. Braasch for mapping some of the trajectories.

REFERENCES

ADVANI, S. & TUCKER, C. L. 1987 The use of tensors to describe predict fiber orientation in short fiber composites. *J. Rheol.* **31**, 751–784.

AIT-KADI, A. & GRMELA, M. 1994 Modelling the rheological behavior of fiber suspensions in viscoelastic media. *J. Non-Newtonian Fluid Mech.* **53**, 65–81.

ALLEN, E. & UHLHERR, P. H. T. 1989 Nonhomogeneous sedimentation in viscoelastic fluids. *J. Rheol.* **33**, 627–638.

ANCZUROWSKI, E. & MASON, S. G. 1968 Particle motions in sheared suspensions. XXIV. Rotation of rigid spheroids and cylinders. *Trans. Soc. Rheol.* **12**, 209–215.

BARTRAM, E., GOLDSMITH, H. L. & MASON, S. G. 1975 Paricle motion in non-Nwtonian media III. Further observations in elasticoviscous fluids. *Rheol. Acta* **14**, 776–782.

BECRAFT, M. L. & METZNER, A. B. 1992 The rheology, fiber orientation, and processing behavior of fiber-filled fluids. *J. Rheol.* **36**, 143–174.

BIRD, R. B., ARMSTRONG, R. C. & HASSAGER, O. 1987 *Dynamics of Polymeric Liquids. Vol. 1: Fluid Mechanics*, 2 edn. John Wiley & Sons.

BRIGHT, P. F., CROWSON, R. J. & FOLKES, M. J. 1978 A study of the effect of injection speed on fiber orientation in simple mouldings of short glass fiber-filled polypropylene. *J. Mater. Sci.* **13**, 2497–2506.

BRUNN, P. 1976 The behavior of a sphere in non-homogeneous flows of a viscoelastic fluid. *Rheol. Acta* **15**, 589–611.

BRUNN, P. 1980 The motion of rigid particles in viscoelastic fluids. *J. Non-Newtonian Fluid Mech.* **7**, 271–288.

CHAN, P. C.-H. & LEAL, L. G. 1977 A note on the motion of a spherical particle in a general quadratic flow of a second-order fluid. *J. Fluid Mech.* **82**, 549–559.

CHOI, H. J., PRIEVE, D. C. & JHON, M. S. 1987 Anomalous lateral migration of a rigid sphere in torsional flow of a viscoelastic fluid – effect of polymer concentration and solvent viscosity. *J. Rheol.* **31**, 317–321.

DINH, S. M. & ARMSTRONG, R. C. 1984 A rheological equation of state for semiconcentrated fiber suspensions. *J. Rheol.* **28**, 207–227.

FENG, J., HU, H, H. & JOSEPH, D. D. 1994 Direct simulation of initial value problems for the motion of solid bodies in a Newtonian fluid. Part 2. Couette and Poiseuille flows. *J. Fluid Mech.* **277**, 271–301.

FENG, J., HUANG, P. Y. & JOSEPH, D. D. 1996 Dynamic simulations of sedimentation of solid particles in an Oldroyd-B fluid. *J. Non-Newtonian Fluid Mech.* **63**, 63–88.

FENG, J., JOSEPH, D. D., GLOWINSKI, R. & PAN, T. W. 1995 A three-dimensional computation of the force and torque on an ellipsoid settling slowly through a viscoelastic fluid. *J. Fluid Mech.* **283**, 1–16.

FORTES, A. F., JOSEPH, D. D. & LUNDGREN, T. S. 1987 Nonlinear mechanics of fluidization of beds of spherical particles. *J. Fluid Mech.* **177**, 467–483.

GAUTHIER, F., GOLDSMITH, H. L. & MASON, S. G. 1971*a* Particle motions in non-Newtonian media I. Couette flow. *Rheol. Acta* **10**, 344–364.

GAUTHIER, F., GOLDSMITH, H. L. & MASON, S. G. 1971*b* Particle motions in non-Newtonian media. II. Poiseuille flow. *Trans. Soc. Rheol.* **15**, 297–330.

GIESEKUS, H. 1981 Some new results in suspension rheology. In *Non-Newtonian Flows* (ed. J. F. Wendt). Von Karman Institute for Fluid Dynamics Lecture Series 1981–6.

HEGLER, R. P. & MENNING, G. 1985 Phase separation effects in processing of glass-bead- and glass-fiber-filled thermoplastic by injection molding. *Polymer. Engng Sci.* **25**, 395–405.

HIGHGATE, D. J. & WHORLOW, R. W. 1968 Migration of particles in a polymer solution during cone and plate viscometry. In *Polymer Systems: Deformation and Flow* (ed. R. E. Wetton & R. W. Whorlow), pp. 251–261. Macmillan.

HILL, C. T. 1972 Nearly viscometric flow of viscoelastic fluids in the disk and cylinder system. II. Experimental. *Trans. Soc. Rheol.* **16**, 213–245.

HUANG, P. Y., FENG, J. & JOSEPH, D. D. 1994 The turning couple on an elliptic particle settling in a vertical channel. *J. Fluid Mech.* **271**, 1–16.

INGBER, M. S. & MONDY, L. A. 1994 A numerical study of three-dimensional Jeffery orbits in shear flow. *J. Rheol.* **38**, 1829–1843.

IVANOV, Y., VEN, T. G. M. VAN DER & MASON, S. G. 1982 Damped oscillations in the viscosity of suspensions of rigid rods. I. Monomodal suspensions. *J. Rheol.* **26**, 213–230.

JEFFERY, G. B. 1922 The motion of ellipsoidal particles immersed in a viscous fluid. *Proc. R. Soc. Lond.* A **102**, 161–179.

JOSEPH, D. D. 1990 *Fluid Dynamics of Viscoelastic Liquids*. Springer.

JOSEPH, D. D., LIU, Y. J., POLETTO, M. & FENG, J. 1994 Aggregation and dispersion of spheres falling in viscoelastic liquids. *J. Non-Newtonian Fluid Mech.* **54**, 45–86.

KARIS, T. E., PRIEVE, D. C. & ROSEN, S. L. 1984*a* Lateral migration of a rigid sphere in torsional flow of a viscoelastic fluid. *AIChE J.* **30**, 631–636.

KARIS, T. E., PRIEVE, D. C. & ROSEN, S. L. 1984*b* Anomalous lateral migration of a rigid sphere in torsional flow of a viscoelastic fluid. *J. Rheol.* **28**, 381–392.

KARNIS, A., GOLDSMITH, H. L. & MASON, S. G. 1966 The flow of suspensions through tubes. V. Inertial effects. *Can. J. Chem. Engng* **44**, 181–193.

KARNIS, A. & MASON, S. G. 1966 Particle motions in sheared suspensions. XIX. Viscoelastic media. *Trans. Soc. Rheol.* **10**, 571–592.

KUBAT, J. & SZALANCZI, A. 1974 Polymer-glass separation in the spiral mold test. *Polymer Engng Sci.* **14**, 873–877.

LEAL, L. G. 1975 The slow motion of slender rod-like particles in a second-order fluid. *J. Fluid Mech.* **69**, 305–337.

LEAL, L. G. 1979 The motion of small particles in non-Newtonian fluids. *J. Non-Newtonian Fluid Mech.* **5**, 33–78.

LEAL, L. G. 1980 Particle motion in a viscous fluid. *Ann. Rev. Fluid Mech.* **12**, 435–476.

LIU, Y. J. & JOSEPH, D. D. 1993 Sedimentation of particles in polymer solutions. *J. Fluid Mech.* **255**, 565–595.

MCCOY, D. H. & DENN, M. M. 1971 Secondary flow in a parallel-disk viscometer. *Rheol. Acta* **10**, 408–411.

MICHELE, J., PATZOLD, R. & DONIS, R. 1977 Alignment and aggregation effects in suspensions of spheres in non-Newtonian media. *Rheol. Acta* **16**, 317–321.

PETIT, L. & NOETINGER, B. 1988 Shear-induced structures in macroscopic dispersions. *Rheol. Acta* **27**, 437–441.

PRIEVE, D. C., JHON, M. S. & KOENIG, T. L. 1985 Anomalous lateral migration of a rigid sphere in torsional flow of a viscoelastic fluid. II. Effect of shear rate. *J. Rheol.* **29**, 639–654.

RIDDLE, M. J., NARVAEZ, C. & BIRD, R. B. 1977 Interactions between two spheres falling along their line of centers in a viscoelastic fluid. *J. Non-Newtonian Fluid Mech.* **2**, 23–35.

SAVINS, J. G. & METZNER, A. B. 1970 Radial (secondary) flows in rheogoniometric devices. *Rheol. Acta* **9**, 365–373.

SCHMIDT, L. R. 1977 Glass bead-filled polypropylene. Part II: mold-filling studies during injection molding. *Polymer Engng Sci.* **17**, 666–670.

TOLL, S. & ANDERSSON, P. O. 1993 Microstructure of long- and short-fiber reinforced injection molded polyamide. *Polymer Compos.* **14**, 116–125.

TREVELYAN, B. J. & MASON, S. G. 1951 Particle motions is sheared suspensions. I. Rotations. *J. Colloid Sci.* **6**, 354–367.

WU, S. 1979 Order-disorder transitions in the extrusion of fiber-filled poly (ethylene terephthalate) and blends. *Polymer Engng Sci.* **19**, 638–650.